JCB Article

An actin molecular treadmill and myosins maintain stereocilia functional architecture and self-renewal

Agnieszka K. Rzadzinska, Mark E. Schneider, Caroline Davies, Gavin P. Riordan, and Bechara Kachar

Section on Structural Cell Biology, National Institute of Deafness and Other Communication Disorders, National Institutes of Health, Bethesda, MD 20892

We have previously shown that the seemingly static paracrystalline actin core of hair cell stereocilia undergoes continuous turnover. Here, we used the same approach of transfecting hair cells with actin–green fluorescent protein (GFP) and espin-GFP to characterize the turnover process. Actin and espin are incorporated at the paracrystal tip and flow rearwards at the same rate. The flux rates (~0.002–0.04 actin subunits s^{-1}) were proportional to the stereocilia length so that the entire staircase stereocilia bundle was turned over synchronously. Cytochalasin D caused stereocilia to shorten at rates matching paracrystal turnover. Myosins VI and VIIa were localized alongside the actin paracrystal, whereas myosin XVa was observed at the tips at levels proportional to stereocilia lengths. Electron microscopy analysis of the abnormally short stereocilia in the shaker 2 mice did not show the characteristic tip density. We argue that actin renewal in the paracrystal follows a treadmill mechanism, which, together with the myosins, dynamically shapes the functional architecture of the stereocilia bundle.

Introduction

How complex organelles or intracellular filament ensembles maintain steady-state structure and function while continuously undergoing renewal is a fundamental question in cellular biology. Hearing and balance depend on sensory hair cells equipped with mechanosensitive, microvilli-like organelles called stereocilia. At the threshold of hearing, stereocilia are capable of detecting displacements on a nanometer scale through mechanically gated channels located at their tips (for review see Hudspeth, 1997). In addition, stereocilia length, bundle shape, and mechanical properties are critical to the frequency selectivity and sensitivity of hair cells. Stereocilia, 30–300 in number, are organized into bundles of precisely specified rows of increasing heights forming characteristic staircase patterns. Mammalian auditory hair cells are terminally differentiated and do not regenerate. Although their stereocilia are exquisitely sensitive to mechanical vibration, orderly structured, and easily damaged by overstimulation, they are maintained in proper working order for a lifetime. Each stereocilium is supported by a rigid paracrystalline array of several hundred parallel, uniformly polarized and regularly cross-linked actin filaments (Tilney et al., 1983). The actin filaments are oriented such that the barbed (plus) ends are at the tips of the stereocilia and the pointed (minus) ends at the base. This organization of actin shares many construction principles with the actin formations in microvilli and filopodia, yet it can be up to 120 μm in length. Because of their size, paracrystalline order of their cytoskeletal core, and their precisely specified staircase bundle organization, stereocilia can be advantageously used as a model to study the renewal process and the role of actin dynamics in a continuously functioning organelle.

Recently, we exploited the preferential localization of the β isoform of actin in the stereocilia to determine the locus of actin polymerization and to assess the degree of actin turnover in fully developed hair cells of the rat organ of Corti (Schneider et al., 2002). Transfecting cells with a DNA construct encoding β actin–GFP and imaging with confocal microscopy, we showed that the stereocilia actin filaments are continuously being turned over. Other recent discoveries using a genetic approach have also lead to an appreciation for unforeseen dynamic mechanisms within the stereocilia bundle. Genetic studies have shown that stereocilia formation and function depend on several novel actin-related proteins, including espin and several unconventional myosins, as mutations in their genes cause hereditary hearing loss by specifically disrupting stereocilia structure. Mutations in

Address correspondence to Bechara Kachar, Section on Structural Cell Biology, National Institute of Deafness and Other Communication Disorders, National Institutes of Health, Bldg. 50/Rm. 4249, 50 South Dr., Bethesda, MD 20892-8027. Tel.: (301) 402-1600. Fax: (301) 402-1765. email: Kacharb@nidcd.nih.gov

Key words: hair cells; myosin XVa; myosin VIIa; espin; hearing

Abbreviations used in this paper: SEM, scanning EM; TEM, transmission EM.

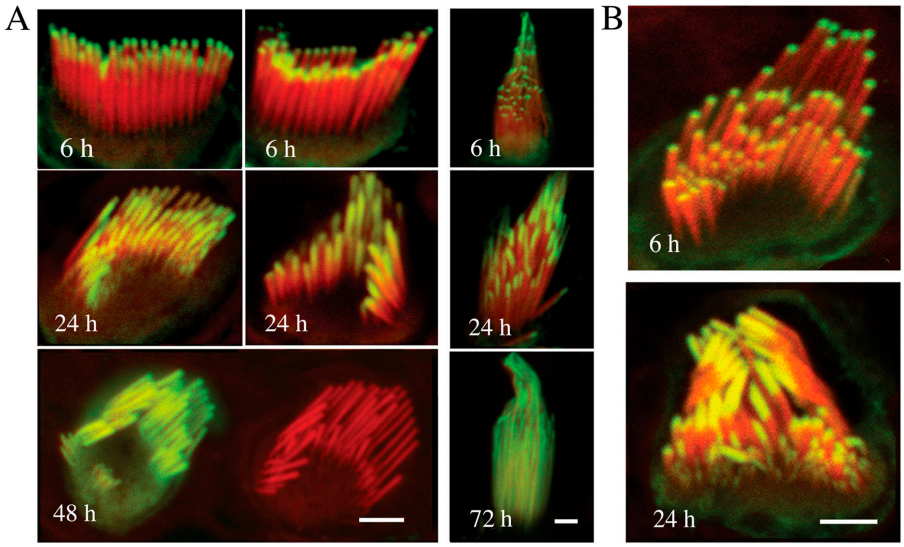

Figure 1. **Incorporation of β actin and espin in stereocilia.** (A) β actin–GFP incorporation into the stereocilia of the hair cells of organ of Corti (left) and vestibular organs (right) after transfection. Confocal microscopy revealed that β actin–GFP (green) appeared at the tips of stereocilia counterstained with rhodamine/phalloidin (red) 6 h after transfection. β actin–GFP was progressively incorporated from the stereocilia tips to their bases within 48 h in the organ of Corti hair cells and within 72 h in the vestibular hair cells. Stereocilia maintained their lengths as evident in the bottom left panel where actin-GFP fluorescence had reached the base of the stereocilia, yet the stereocilia length is similar to the neighboring nontransfected cell. Bars, 2.5 μm. (B) Espin-GFP incorporation into the stereocilia of the hair cells of organ of Corti. Espin-GFP incorporation began at the tips of stereocilia and was progressively incorporated into stereocilia at similar rates as the β actin–GFP shown in A. Bar, 2 μm.

espin, an actin cross-linking protein, cause stereocilia to shorten and lose stiffness (Zheng et al., 2000); mutations in myosin XVa result in very short stereocilia; mutations in myosin VIIa lead to progressive disorganization of the stereocilia bundle; and mutations in myosin VI lead to stereocilia fusion (Steel and Kros, 2001). How stereocilia are formed and maintained while continuously functioning remains a fundamental question in inner ear research.

In this paper, we show that the actin paracrystal renewal process is organized as a "molecular conveyor belt" that mimics "treadmilling," a dynamic behavior of polarized polymers characterized by a net assembly at one end and disassembly at the other while maintaining steady-state length (Wanger et al., 1985). In the proposed stereocilia treadmill model, actin monomers are added at the tips and removed at the base of the stereocilia while the entire paracrystal moves basally. We show that espin is also incorporated at the tip of the stereocilia and moves rearwards at the same rate as actin. Most importantly, the treadmilling of the stereocilia paracrystal is highly regulated and the treadmill rates are scaled to the stereocilia length. We also characterize the localizations of myosins XVa, VIIa, and VI in relation to the actin paracrystal using light and electron microscopy immunolocalization techniques. We show that myosin XVa is localized at the barbed ends of the actin filaments of the paracrystal, whereas myosins VI and VIIa are localized alongside the paracrystal. We also show that the immunoreactivity levels for myosin XVa are proportional to the length of the stereocilia. The presence of these myosins at the tip and along the actin paracrystal suggests that they could be involved in paracrystal dynamics and stereocilia plasticity. Recognition of the dynamic nature of a structure previously regarded as the epitome of a stable cellular ensemble because of its ordered structure and mechanosensitivity is essential to understanding the development, repair, and maintenance of normal sensory function.

Results

Actin renewal is common to all hair cell stereocilia

We studied the incorporation of β actin–GFP into stereocilia in organotypic cultures of hair cells from rat and mouse inner ear sensory epithelia. In mice and rats, stereocilia progressively emerge from the surface of hair cells, form a staircase bundle, and start exhibiting mechanosensitivity (Kennedy et al., 2003) and attain adult size (Romand et al., 1993) by postnatal days 5–7. In our experiments, hair cell cultures were transfected with a β actin–GFP at postnatal days 7–10 and analyzed up to postnatal day 15. Samples were fixed at specific time points and actin filaments were counterstained with rhodamine/phalloidin and examined with confocal microscopy. Incorporation of β actin–GFP into the actin core begins at the tips of stereocilia as early as ∼5 h after transfection in all hair cell types, including inner and outer hair cells of the organ of Corti and hair cells from all three vestibular organs (Fig. 1 A). Actin-GFP fluorescence progresses toward the base. Auditory hair cells from the middle turns of the organ of Corti synchronously renew about half the length of their stereocilia in 24 h and complete their renewal within 48 h. The actin-GFP fluorescence pattern grows toward the base, whereas the lengths of the stereocilia remain constant. This effect is particularly evident after 48 h of transfection when the stereocilia are entirely labeled and their length remains the same as that of the stereocilia of neighboring nontransfected cells (Fig. 1 A). We did not detect any increase in the overall length of the stereocilia at any of the observation times after transfection of hair cells from all turns of the organ of Corti. A similar process of actin incorporation and flux takes place in the vestibular hair cells, but it takes ∼72–96 h for their much longer stereocilia to show actin-GFP along the entire stereocilia (Fig. 1 A). The results for mouse (unpublished data) and rat tissues appeared consistently similar, but because the rat hair cell stereocilia are larger and easier to visualize, we focused the majority of our analyses and figure illustrations on rat hair cells.

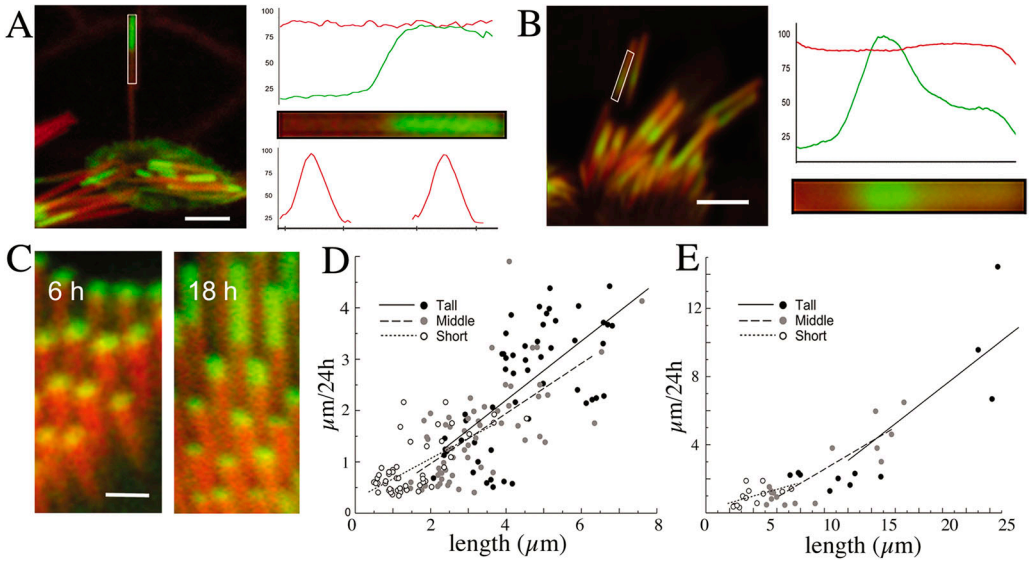

Figure 2. **Characterization of the actin incorporation and flux.** (A) Characterization of actin-GFP incorporation into the stereocilia actin paracrystal. The pixel intensity profile along an individual stereocilium (rectangular area) shows the sharp demarcation of the β actin–GFP incorporation (green), whereas the pixel intensity of the rhodamine/phalloidin counterstained actin filaments (red) shows a constant profile. The pixel intensity from the rhodamine/phalloidin shows the same profile when measured across the region of β actin–GFP incorporation or across the region without actin-GFP, excluding the possibility that incorporation was due to nucleation of additional actin filaments. Bar, 2 μm. (B) Transient β actin–GFP expression in an auditory hair cell. The serendipitous pulse of actin-GFP (green) expression was arrested midway along the stereocilia (left). The incorporation appears as a band that has progressed halfway along the stereocilia showing a sharp front facing the stereocilia base (similar to the stereocilia in C) and a diffuse attenuated trailing edge facing the tip. It also shows no change in the total actin fluorescence along the stereocilia, confirming that no anomalous actin filaments are added laterally to the actin paracrystal. Bar, 2 μm. (C) The extent of actin incorporation and treadmill rates is proportional to the length of the stereocilia in a bundle. Even at the earliest times of transfection, we could detect in the fluorescence confocal images that the actin-GFP incorporation starts at the same time in all stereocilia in a bundle but the rate of incorporation and subsequent actin treadmilling are proportional to the stereocilia length in both organ of Corti (left, 6 h after transfection) and vestibular (right, 18 h after transfection) hair bundles. Bar, 600 nm. (D and E) Relationship of the treadmill rates to the length of the stereocilia. The overall actin-GFP treadmill rates calculated by measuring lengths of incorporation 12–24 h after actin-GFP transfection and expressed as μm/24 h for the organ of Corti (D) and vestibular (E) stereocilia. The rate of actin treadmill is proportional to the length of the stereocilium irrespective of its rank (tall, middle, or short) within the staircase bundle.

Stereocilia espin is renewed at the same rate and pattern as actin

Because the actin filaments of the stereocilia are cross-linked into a rigid paracrystalline structure, we investigated the dynamics of a protein involved in cross-bridging in relation to actin renewal. Espin, a potent actin bundling protein, is critical for normal stereocilia structure (Zheng et al., 2000) and, as observed by immunoelectron microscopy, is uniformly distributed along the entire length of the stereocilia (unpublished data). We transfected hair cells with an espin-GFP construct using the same transfection procedure used for the β actin–GFP and tracked its rate and pattern of incorporation. As previously shown, transfections with this plasmid can rapidly result in espin overexpression (Chen et al., 1999). In cases with limited espin-GFP expression, incorporation also started at the tips of stereocilia and its fluorescence pattern extended toward the base with a similar rate and order as that seen for β actin–GFP incorporation and flux for auditory (Fig. 1 B) and vestibular hair cells (not depicted). We did not observe espin incorporation in these stereocilia at regions other than at the tips, indicating that unless it is overexpressed, espin does not bind preformed actin filaments. However, after 24 h of transfection in all cells we observed, espin-GFP overexpression induced the formation of anomalous espin cross-linked actin bundles throughout the cytoplasm (unpublished data) similar to the anomalous actin bundles previously reported in espin-transfected cultured cell lines (Chen et al., 1999).

Characterization of the actin flux

To exclude the possibility that the observed actin incorporation and flux is a result of anomalous actin overexpression or a de novo nucleation of additional actin filaments at the actin paracrystal circumference, we analyzed the actin distribution by measuring pixel intensities in the fluorescence image. We used rhodamine/phalloidin to counterstain all the actin filaments and compared the fluorescence intensity profile measured along and across the stereocilia over the region where actin-GFP was incorporated. As shown in Fig. 2 A, such analysis shows that actin-GFP marks have a sharp leading edge, indicating that incorporation and flux is uniform for all filaments in the paracrystal. Also, there is no increase in rhodamine fluorescence across the region where actin-GFP is incorporated that would indicate formation of additional filaments laterally to the paracrystal (Fig. 2 A). Additional evidence illustrating the pattern of actin incorporation and flux was observed after serendipitous attenuation of β actin–GFP expression (Fig. 2 B). In this case, the incorporation appears as a band that has progressed halfway along the stereocilia. This band shows a sharp front facing

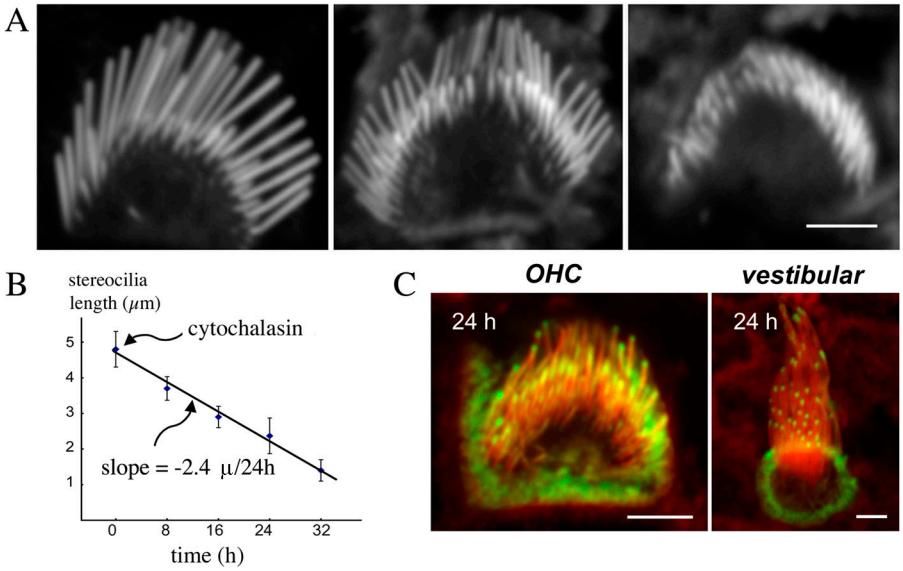

Figure 3. **Effects of cytochalasin D on stereocilia.** (A) Cytochalasin D shortens stereocilia as it blocks actin polymerization. Confocal images of phalloidin-stained stereocilia of representative hair cells after 1-μM cytochalasin D treatment of middle turn cochlear cultures (n = 10) indicate that stereocilia progressively decrease in length. All cells in the culture demonstrated stereocilia shortening over time without apparent change in the staircase pattern of the hair bundle. Bar, 2.5 μm. (B) The rate of stereocilia shortening is linear and matches the rate of actin polymerization. The lengths of the tall row of stereocilia were measured at 8-h intervals after 1 μM cytochalasin treatment, and the average values ± SD (n = 50) were plotted in the graph. The slope of the best-fit curve indicates an actin shortening rate of 2.4 μm/24 h. (C) Cytochalasin inhibits actin-GFP incorporation. Representative confocal images (n = 30 cells) of stereocilia from the apical turn of the organ of Corti (left) and vestibular (right) hair cells showing actin-GFP marks that have been incorporated for 8 h into the paracrystal. Actin-GFP marks remained at the tips and did not increase in length or progress down the stereocilia over the ensuing 16 h after the incubation with cytochalasin. Bars: (left) 2.4 μm; (right) 1.5 μm.

the stereocilia base and a diffuse attenuated trailing edge facing the tip as incorporation of GFP-labeled actin is gradually reduced in favor of unlabeled actin. It also shows no change in the total actin fluorescence along the stereocilia, confirming that no anomalous actin filaments are added laterally to the actin paracrystal.

The overall rate of the actin incorporation is matched to the length of the stereocilia

We calculated the rates of actin flux in stereocilia by measuring the lengths of the β actin–GFP incorporation marks and stereocilia lengths. In each bundle, the rate of the actin-GFP incorporation/flux was relatively constant for stereocilia of the same length within a row. However, each row of stereocilia in the bundle exhibited a different incorporation rate (Fig. 2 C). To evaluate the relationship between incorporation/flux rate and stereocilia length, we calculated the flux rates in stereocilia from different rows (tall, middle, and short) in hair cells from all regions of the organ of Corti (Fig. 2 D) and vestibular organs (Fig. 2 E). Actin flux rates (μm/24 h) were measured at 18–24 h after transfection. The flux rates within a bundle appear to be scaled to the length of the stereocilia such that the longest stereocilia exhibit the fastest rates. Also, in the organ of Corti, the rates of actin flux are tonotopically organized such that the fastest rates are observed in the longer stereocilia of the apical region of the cochlea. Overall, the flux rate varied from ∼0.9 μm/24 h in the short stereocilia to ∼2.8 μm/24 h in the long stereocilia. The flux rates for the vestibular stereocilia ranged from ∼1 μm/24 h in the shorter (∼4 μm) to ∼5 μm/24 h in the longer (∼20 μm) stereocilia. The scaling of the flux rate to the length of the stereocilia indicates that the residence time for each actin subunit or espin molecule in each stereocilium in a bundle is approximately the same and independent of the length. Consequently, all the stereocilia in a bundle undergo total renewal of their actin paracrystal within the same time interval of ∼2 d for the organ of Corti hair cells and ∼3–4 d for the vestibular hair cells.

Cytochalasin D shortens stereocilia as it blocks actin polymerization

To evaluate the contribution of actin polymerization to the incorporation and flux mechanisms and the maintenance of stereocilia length, we analyzed stereocilia exposed to the actin polymerization inhibitor cytochalasin D. We applied 1 μM cytochalasin D to 7-d-old cultures from all regions of the cochlea, fixed the preparations at 8, 16, 24, and 32 h, and analyzed the stereocilia lengths. We observed a progressive reduction in stereocilia lengths without significant changes in the characteristic structure of each stereocilium and staircase organization of the bundle (Fig. 3 A). We measured the length of stereocilia from the tallest rows in the bundles of inner and outer hair cells from the middle turns of organ of Corti and plotted the length as a function of time (Fig. 3 B). The estimated rate of shortening was 2.4 μm/24 h. Next, we assessed if actin-GFP marks that have been incorporated into the paracrystal continue to move after assembly is blocked during the shortening process. We repeated the cytochalasin D experiment with stereocilia labeled with β actin–GFP for 8 h before the drug application. We observed (n = 30 cells) that the actin-GFP marks remained at the tips and did not increase in length or progress down the stereocilia over the ensuing 16 h after the incubation with cytochalasin (Fig. 3 C).

How tightly regulated is the stereocilia length?

Images of fully formed bundles from in vivo tissues show that although there is an overall uniformity of length, stereocilia of the same ranks within the bundle staircase still exhibit slight individual variations (Fig. 4, A and B). These slight variations in length, which are more pronounced in vestibular hair cells, are also evident in chick hair cells (Til-

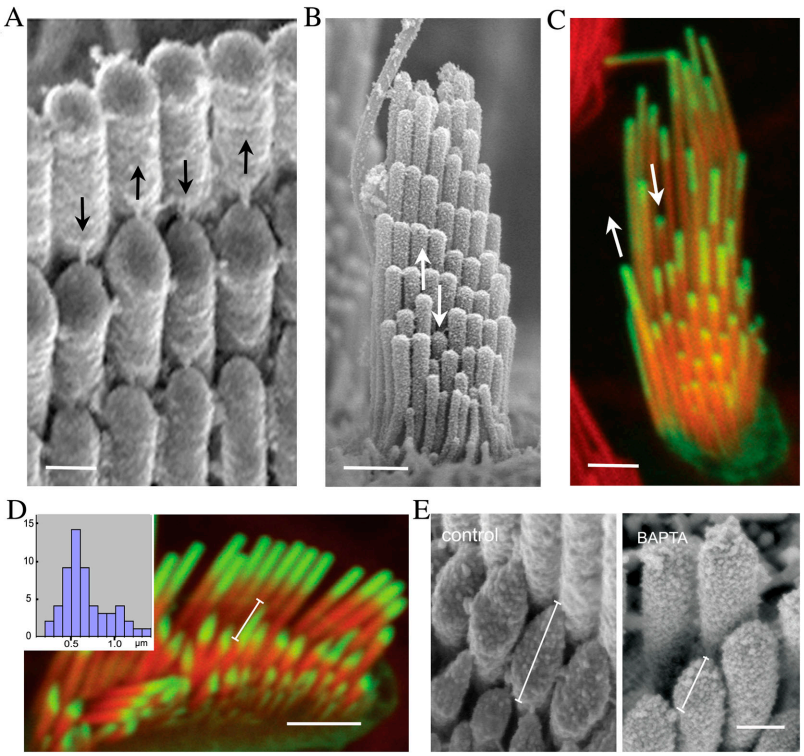

Figure 4. **Dynamic regulation of stereocilia structure.** (A–C) SEM images of organ of Corti (A) and vestibular (B) hair bundles demonstrate slight irregularities in stereocilia lengths within the characteristically packed rows of the hair bundle. Arrows pointing down show slightly shorter stereocilia, whereas arrows pointing up show longer stereocilia in the same row. In the actin-GFP–transfected vestibular hair cell, the incorporation and treadmill rates (C) reflect the slight length variations within stereocilia of the same row in the bundle. The actin treadmill rates are faster in stereocilia that are taller than their neighbors in the same row (upward arrow) and slower in stereocilia that are shorter than their peers of the same row (downward arrow). Bars: (A) 250 μm; (B) 1 μm; (C) 2 μm. (D) Natural variability in stereocilia tip shape and rate of actin-GFP incorporation. The stereocilia of the tallest row in a bundle have uniform oblate tips, whereas the stereocilia from the second and lower rows exhibit prolate tips that can be slightly pointed to very elongated. The rate of actin-GFP incorporation is increased in the more elongated tips. Bar, 2 μm. Inset shows the frequency distribution of tip length measured as indicated by the measuring bar in the figure. (E) Remodeling of stereocilia tips exposed to BAPTA. SEM images of the stereocilia after 5-min incubation with 5 mM BAPTA in calcium-free L-15 media and 30-min recovery (right) reveal that tip links are disrupted and stereocilia tips become rounded when compared with control (left). The length of the tip defined as shown on the figure was 0.51 ± 0.05 μm for control and 0.34 ± 0.02 μm for BAPTA-treated stereocilia (n = 50). Bar, 250 nm.

ney et al., 1983) and were observed in our cultured hair cells (Fig. 4 C). Correlating with these length variations is the observation that stereocilia of the same ranks also show slight variations in the actin incorporation rates. Within the same ranks, stereocilia that are shorter than their neighbors show a slower rate of actin-GFP incorporation, whereas those that are longer show an accelerated incorporation (Fig. 4 C, arrows). We observed that pronounced irregular lengths and rates of incorporation occurred more frequently when the stereocilia appeared displaced from the regular staircase organization. These results indicate that fluctuations of actin incorporation rates produce transient net gain or net loss of actin core length and that the overall stereocilia lengths are constantly modulated.

The role of tip links on the length and shape of stereocilia tips

We observed that the shape of the tip of the stereocilia in vivo, in particular in the organ of Corti, exhibits a structural polymorphism that appears to be related to tension on the tip link. Although the stereocilia of the tallest row have a characteristic oblate tip, the stereocilia of the second and lower rows typically have an asymmetrical prolate tip that points toward their taller neighbor (Fig. 4). These pointed tips seem to conform to the structural presence and mechanical pull of the putative tip link. A close-up view of the actin-GFP incorporation after a short period of transfection shows that the stereocilia from the second and lower rows exhibit variability in both the rate of actin-GFP incorporation and also variability in the shape of their prolate tips (Fig. 4 D). The highest rates are observed in the more elongated and sharply pointed tips. This raises the possibility that transient fluctuations of the rate of actin polymerization resulting in transient net gain or loss in length are induced or modulated by tip link tension or gating of the transduction machinery.

To test if the pointed tips are indeed correlated to the presence of intact tip links and if they could remodel after tip link loss, we treated cultures with a transient exposure to BAPTA, a calcium chelator known to disrupt tip links and mechano-transduction of hair cells (Assad et al., 1991). We analyzed changes of stereocilia tip shape both by light microscopy and by scanning EM (SEM). We observed that when the tip links are disrupted by BAPTA, the tips of the second and lower rows of stereocilia progressively attenuate their sharp pointed ends and assume a more rounded shape within 30 min after the BAPTA treatment (Fig. 4 E). To quantify this remodeling, we estimated the average length of the tip of the stereocilia (n = 30) to be 0.55 ± 0.03 μm in the control samples and decrease to 0.34 ± 0.02 μm after the BAPTA treatment (Fig. 4 E). This observation strongly suggests that the presence of the tip link may dynamically influence the shape of the stereocilia tip and its actin paracrystal core. Interestingly, close inspection of previously published images of BAPTA-treated stereocilia of chick hair cells show similar progressive rounding of the stereocilia tip (Kachar et al., 2000), suggesting that this phenomenon is common to all stereocilia.

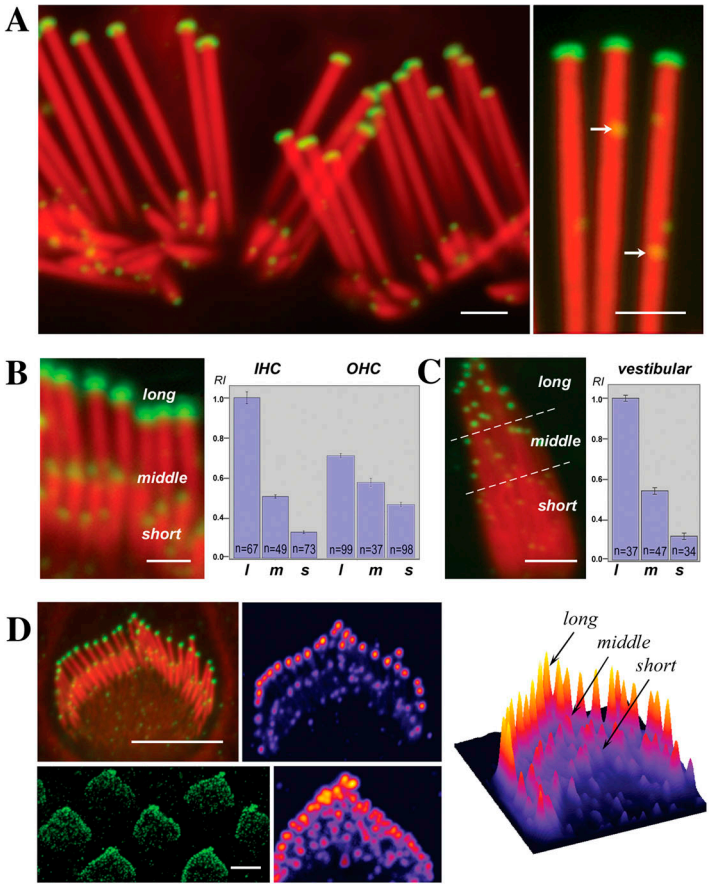

Figure 5. **Intensity of myosin XVa labeling in the tips of stereocilia is graded with length.** (A–C) Myosin XVa is localized to the stereocilia tips of auditory (A and B) and vestibular (C) hair cells. Confocal images revealed myosin XVa immunofluorescence in all stereocilia tips of the rat auditory hair cells (A) and at higher magnification also exhibited small fluorescence puncta (A, right, arrows) along the entire stereocilia. Levels of myosin XVa labeling are highest in the longest stereocilia within the auditory (B) and vestibular (C) hair bundle. The relationship between myosin XVa and stereocilia length is visible in fully developed bundles (A) as well as in cultured auditory (B) and vestibular hair cells (C). Quantitative analysis of average pixel intensity confirms myosin XVa gradation within hair bundles of inner (IHC) and outer (OHC) auditory hair cells (B) as well as vestibular hair cells (C). Error bars equal mean ± standard error of the mean. l, long; m, middle; s, short stereocilia. The gradient of myosin XVa expression is noticeable at the earliest stages of the staircase formation in inner (D, top) and outer (D, bottom) hair cells from postnatal day 1 rat neonates whose shorter stereocilia are indistinguishable from supernumerary microvilli. Scaling of myosin XVa levels to the stereocilia length and their distribution within a bundle is clearly visible on the pseudo-colorized images and surface plot of pixel intensities (D); the highest intensities are shown in red. Bars: (A and B) 1 μm; (C) 2 μm; (D) 4 μm.

Myosin XVa immunoreactivity at stereocilia tips is scaled to their lengths

Abnormally short stereocilia are observed in the shaker 2 and 2J mice, which carry mutations on the motor and FERM domains of myosin XVa, respectively (Anderson et al., 2000). Myosin XVa is an unconventional myosin suggested to have a role in the formation of stereocilia. To extend previous results on the localization of myosin XVa in hair cells and to gain insight into its role in stereocilia actin dynamics, we analyzed its precise localization using immunofluorescence. We observed intense and well-localized fluorescence signals at the stereocilia tips in whole-mount preparations of adult mouse, rat, and guinea pig organ of Corti and vestibular sensory epithelia using two affinity-purified antibodies. Virtually all stereocilia had detectable levels of myosin XVa labeling at their tips (Fig. 5 A). Moreover, although the primary localization of myosin XVa was at the tips of the stereocilia, occasional fluorescence puncta were also visualized along the stereocilia (Fig. 5 A). Detailed analysis of the fluorescence image revealed that the levels of myosin XVa fluorescence signal are scaled to the stereocilia length (Fig. 5). In both auditory and vestibular hair cells, the highest levels of fluorescence were observed in the tallest stereocilia of the bundle, whereas stereocilia of the second and lower rows showed considerably lower levels. We extended these immunofluorescence studies to embryonic and early postnatal stages of rat inner ear development to determine when the gradation in myosin XVa immunofluorescence signal arises. We detected myosin XVa signals at the tips of the earliest observable stereocilia on the surface of hair cells in embryonic day 18 cochlea. The gradation in myosin XVa fluorescence levels between different stereocilia rows was noticeable from the earliest emergence of nascent supernumerary stereocilia (Fig. 5 D).

Myosin XVa is a component of the electron-dense structure at the stereocilia tip

The shape of the tips of the taller and shorter stereocilia and the localization of myosin XVa are more clearly visualized by transmission EM (TEM) of fast-frozen, freeze-substituted specimens. Fast freezing optimally preserves both the actin filaments and the stereocilia membrane and distinctly differentiates the oblate tips of the taller stereocilia from the asymmetric prolate tips of the shorter stereocilia (Fig. 6). In all stereocilia, the actin filaments are graded in height such that they terminate on the dome- or conical-shaped membrane. The TEM images also show that the membrane at the tip of the stereocilia is subtended by an electron-dense structure, which has been previously reported as an osmiophilic structure covering the tips of the actin filaments in conventionally fixed tissues (Fig. 6, A and B, middle). This dense structure covers the entire oblate dome at the top of the taller stereocilia. In the shorter stereocilia, a smaller densely stained patch covers only the most distal part of the prolate asymmetric tip in the region of tip link insertion. The tallest stereocilia show very strong myosin XVa staining covering their oblate tips (Fig. 6 A). Conversely, myosin XVa staining of the shorter stereocilia is restricted only to a small and elongated patch on the most distal end of their prolate tips (Fig. 6 B). The im-

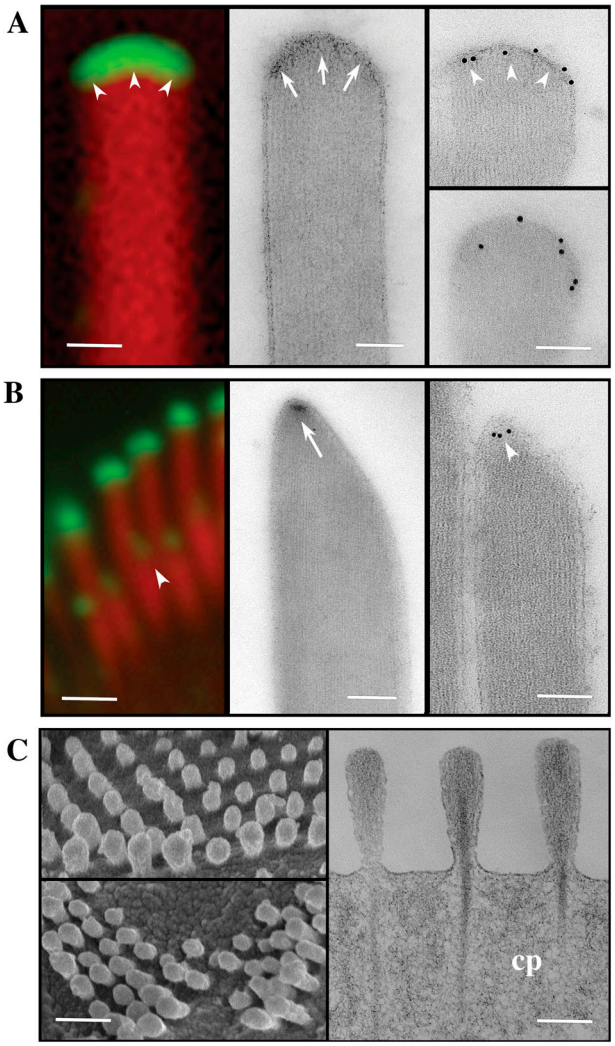

Figure 6. **Myosin XVa is a component of the stereocilia tip complex.** (A and B) Comparison of high magnification confocal immunofluorescence (left), TEM of uranyl acetate–stained sections (middle), and immunogold-labeled unstained sections (right) of the oblate (A) and prolate (B) stereocilia tips. Stereocilia tips of the tallest row of the bundle are prolate in shape with an electron-dense region just below the stereocilia membrane (A, arrows), where intense myosin XVa labeling is visualized by immunofluorescence or by immunogold EM (A, arrowheads). The second row stereocilia in the bundle are prolate and pointed (B) with a smaller discrete electron-dense region at the end of their longest actin filaments (B, arrow), which also coincides to where myosin XVa is visualized by either fluorescence or by immunogold EM (B, arrowheads). (C) SEM images of shaker 2J mutants confirm previous observations that stereocilia, despite being very short, maintain a slight length gradation reminiscent of the staircase pattern of a normal hair bundle. TEM of osmium and uranyl acetate–stained thin sections (right) show that these very short stereocilia maintain the overall organization of the actin filaments including the rootlets that insert into the cuticular plate (cp) but their tips lack the electron-dense material seen in normal stereocilia (A and B). Bars: (A) 100 nm; (B) 1 μm (left) and 100 nm (right); (C) 1 μm (left) and 100 nm (right).

munogold labeling precisely correlates with the immunofluorescence. Moreover, as seen in the fluorescence data and by immunogold labeling (Fig. 6, A and B), it is qualitatively evident that the immunolocalization level for myosin XVa is also graded within the bundle staircase.

It was previously reported that myosin XVa expression is not detectable in the abnormally short stereocilia in shaker 2 and 2J mice (Anderson et al., 2000). To characterize the structural changes to the tips of stereocilia that accompany the absence of myosin XVa, we performed a combination of SEM and TEM analyses of shaker 2J mice stereocilia. These very short stereocilia show some rudiments of the staircase-like graded heights but do not show tip link or lateral link connections (Fig. 6 C) that are hallmark structures in normal stereocilia. In addition, we observed that all stereocilia tips show a symmetrically rounded shape and lack the electron-dense structure at the end of the actin paracrystal.

Myosins VI and VIIa immunoreactivity alongside the actin paracrystal

Myosins VI and VIIa are two other unconventional myosins highly expressed in hair cells (Hasson et al., 1997). To determine if these other myosins also localize to the tips of stereocilia we investigated their pattern of localization. We found that whereas myosin XVa is predominantly localized to the tips of stereocilia, myosins VI and VIIa are virtually excluded from this region but are consistently localized between the actin core and the lateral membrane (Fig. 7).

Discussion

Actin polymerization and paracrystal assembly at the stereocilia tip

The observation that incorporation of actin monomers occurs at the tips of the stereocilia at the barbed (plus) end of the paracrystal actin filaments is consistent with the known property of actin filaments to elongate by the preferential incorporation of actin monomers to the barbed end. In order for the newly polymerized actin filament to assemble into a uniform actin paracrystal, the regular cross-bridging must also occur in step with the actin polymerization process. We have observed that actin monomers as well the cross-linking protein espin are incorporated at the stereocilia tip and progress toward the base at the same flux rates. We did not detect espin incorporation at regions other than at the site of paracrystal assembly. Polymerization and cross-linking could in fact be tightly "coupled." A similar coupling of polymerization and cross-linking was suggested for the in vitro formation of actin-fimbrin bundles where it was shown that the paracrystalline organization could not be assembled simply from preformed actin filaments by adding diffusible cross-bridging proteins (Volkmann et al., 2001). The preferential incorporation of espin at the tips of the stereocilia and in step with the actin polymerization is consistent with this possibility.

Actin depolymerization and paracrystal disassemble at the stereocilia base

Stereocilia are anchored at their base to the cuticular plate, a network of crisscrossed and branched actin filaments. At the base of the stereocilia, the actin paracrystal is tapered and the majority of filaments terminate in close apposition to the plasma membrane, leaving only the central filaments of the paracrystal to insert in the cuticular plate (Tilney et al., 1983). Our observation that incorporation and flux of actin-

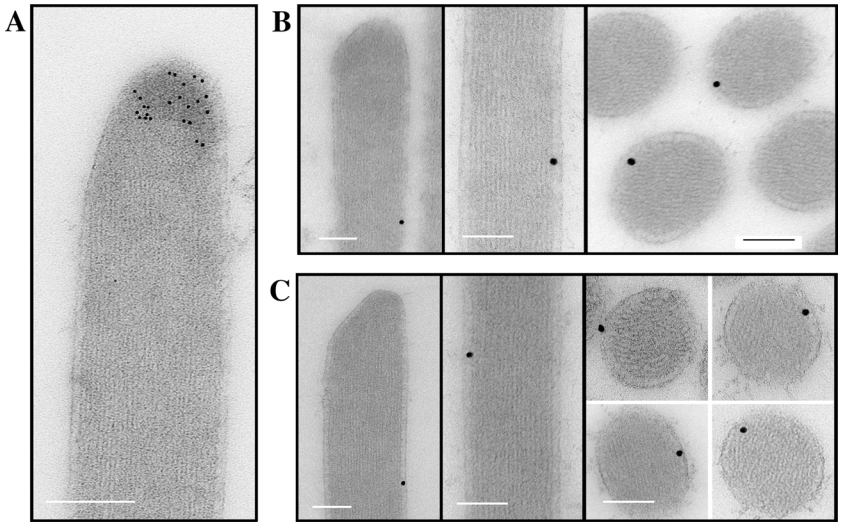

Figure 7. **Comparative localization of myosins XVa, VI, and VIIa in vestibular hair cell stereocilia.** Immunogold labeling of vestibular hair cell stereocilia showing myosin XVa at the stereocilia tip region (A) while myosins VI (B) and VIIa (C) were localized between the actin core and the lateral membrane as seen in longitudinal and cross-sections. Bars, 100 nm.

GFP occurs continuously and uniformly from the tips to the base, whereas the stereocilia and cuticular plate maintain steady-state structure, strongly suggests that the paracrystal is disassembled at the base and the actin filaments are depolymerizing at their pointed end. The observation that stereocilia shortening and rearward movement of the actin-GFP marks when polymerization is blocked by cytochalasin D is consistent with this interpretation.

How does actin flow from the tip to the base of the stereocilia?

The entire process of assembly, rearwards flux, and disassembly has several parallels to a process termed treadmilling. Treadmilling has been described as a system where a polarized polymer (or population of polymers) exists in a steady state characterized by net plus end assembly and minus end disassembly. This results in plus-to-minus end-directed subunit flux through polymer. In an actin filament treadmill model (Wanger et al., 1985), monomers are continuously added to the filament barbed (plus) end and removed from its pointed (minus) end while the filament maintains constant length in a dynamic steady state. We believe that paracrystal assembly and subunit flux in the stereocilia follow a treadmill model as shown in Fig. 8 A. We base this interpretation and our model on the following observations: (a) we show a flux of labeled actin from the barbed to the pointed end as the actin filament paracrystal maintains constant length; (b) actin overexpression does not drive an increase or decrease of the length of the actin paracrystal; (c) there is no evidence for the addition of actin filaments to the periphery of the actin paracrystal; (d) when the polymerization is inhibited with cytochalasin D, the transient actin-GFP marks do not grow but continue to move down as the stereocilia shorten; and (e) the rate of shortening or depolymerization in the cytochalasin-treated stereocilia is equivalent to the rate of actin polymerization/flux in the untreated stereocilia when the length is maintained constant. We interpret the actin flux measured in the stereocilia as the paracrystal treadmilling rate in the unique special case where the lengths of the stereocilia are held constant.

Intrinsic factors influencing treadmill rates

Assuming that all filaments in an actin paracrystal treadmill at the same rate, the fastest actin flux rates of ~5–10 μm/24 h observed in the longest stereocilia correspond to ~0.02–0.04 subunits (per filament) per second. The overall range we observed from the slowest to the fastest was from ~0.004 to 0.04 s^{-1}. It is interesting to note that our fastest rates are within an order of magnitude of treadmilling rates observed for individual actin filaments in an in vitro system (Wegner, 1976; Fujiwara et al., 2002). The rates of actin flux observed in parallel actin bundles of microvilli and filopodia are up to 100 times faster (Mallavarapu and Mitchison, 1999; Tyska and Mooseker, 2002; Loomis et al., 2003). Several factors could influence the flux rates in stereocilia by affecting the assembly and/or disassembly processes. The parallel actin bundles of stereocilia, microvilli, and filopodia differ by the degree and nature of their cross-bridging. In stereocilia, over 200 actin filaments are tightly packed to form a paracrystal by espin and fimbrin, whereas in microvilli, ~20 actin filaments are loosely cross-bridged by fimbrin (for review see Bartles, 2000). We speculate that the extensive fimbrin and espin cross-linking in the stereocilia paracrystal may slow down actin disassembly. Recent works on similar parallel actin bundles in *Drosophila melanogaster* bristles show that stability and turnover of the actin bundle is related to the number and nature of cross-bridges (Tilney et al., 2003). How the actin flux rates are regulated in the stereocilia actin paracrystal is an important unsolved issue.

Treadmilling versus retrograde flow

In some cases, treadmilling has been shown to coexist with actions of a molecular motor (like a myosin), which exerts translocation force on the polymer(s) as they treadmill. Motor presence may affect either or both polymer dynamics and polymer translocation. Rearward movement of actin cytoskeletal assemblies assisted by myosins has been termed "retrograde flow" (Forscher et al., 1987), which has been described in systems with a very dynamic cytoskeletal/membrane framework often undergoing movements of extension and retraction against a rigid substrate. We cannot exclude the possibility that the rearward movement of the actin paracrystal is

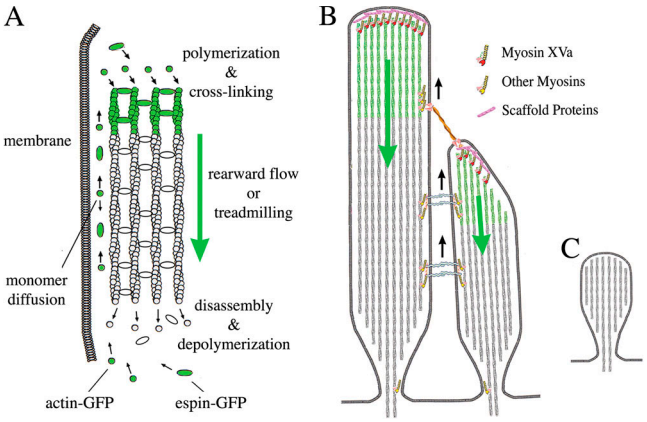

Figure 8. **An actin molecular treadmill model for the dynamic regulation of stereocilia functional architecture.** (A) Diagram illustrating the actin paracrystal treadmill model. Actin polymerization and espin cross-linking into a paracrystal occur at the barbed (plus) end of actin filaments near the stereocilia tip complex. Paracrystal disassembly and actin filament depolymerization occurs at the pointed (minus) end of actin filaments at the base of the stereocilia. When the rate of assembly at the tips is equivalent to the rate of disassembly at the base, the paracrystal undergoes a rearward flow or treadmilling and the paracrystal length is dynamically maintained constant. (B) Diagram of a longitudinal section view of two neighboring stereocilia linked by tip and lateral links illustrating the localization and possible relationship of myosins to the actin paracrystal treadmill. Actin flux or treadmill in each stereocilia is independently regulated. Myosin XVa localized to the stereocilia tip complex could regulate or coordinate actin polymerization and/or paracrystal assembly. Tip link tension may regulate the stereocilia tip complex and actin incorporation in the shorter stereocilia. Other myosins localized lateral to the paracrystal may have a role in retrograde flow or dynamic positioning the stereocilia links along the paracrystal treadmill. (C) Diagram illustrating the shaker 2J mutant mice stereocilia, which are abnormally very short, have a rounded tip, and lack myosin XVa and the electron-dense structure or tip complex.

somehow assisted by myosins in a retrograde flow type movement. However, it is not clear how this would occur in the particular case of the stereocilia. Myosin VIIa located alongside the stereocilia paracrystal would be in a position to produce force between the paracrystal and the membrane. However, because the stereocilia are not attached to a substrate laterally, a myosin bridging the paracrystal and the membrane could not exert an effective action on the paracrystal unless the membrane is maintained under tension. Therefore, it remains to be determined how much of the rearward movement of the paracrystal is driven by a treadmill-type process and how much is driven by the action of myosins in a retrograde flow process against a tensed encapsulating membrane.

Is actin filament elongation influenced by tension on the stereocilia membrane?

Except for a very narrow neck at the tapered base that allows the central actin filaments to anchor to the cuticular plate, the entire paracrystal actin core is contained within the encapsulating stereocilia membrane. Therefore, membrane tension or variations on the tension could have an effect on the paracrystal structure and dynamics. An indication that the stereocilia-encapsulating membrane is under positive tension is seen in EM images of stereocilia obtained by freeze etching (Kachar et al., 2000) or thin sections as shown in Fig. 5. These images show the encapsulating membrane with a smooth profile consistent with a tensed membrane and gradation of the actin filament lengths that precisely matches the membrane profile. In order for the actin filaments to display such ordered gradation in lengths, the actin elongation process must directly or indirectly be influenced by the compressive force normal to the membrane tension. Moreover, actin polymerization and elongation at the ends of each filament would exert a reciprocal force on the membrane and influence its shape (Mogilner and Oster, 1996). In such a model, actin polymerization would stall at a certain level of balance between the opposing forces produced by the membrane tension and the actin polymerization. This reciprocal relationship between the actin polymerization and the membrane tension can be adjusted toward a net gain or net loss and help define the length and shape of the stereocilia tip. Tip links can directly influence membrane tension by pulling from the extracellular side of the membrane. Our experiment with BAPTA is consistent with this possibility. The disruption of the tip link with BAPTA and subsequent retailoring of actin filaments and progressive rounding of the stereocilia tips supports the hypothesis that membrane tension can influence actin incorporation. However, we cannot exclude that other signaling mechanisms such as Ca^{2+} entry through the transduction channel could also be involved.

Regulation of stereocilia length

Our data clearly demonstrate that treadmill rates are scaled to the lengths of the stereocilia in the bundle and that this process is dynamically regulated. To maintain the steady-state length of the stereocilia paracrystal, the two processes, assembly and disassembly, must be precisely matched. Treatment with cytochalasin D uncouples the two processes and results in the progressive shortening of the stereocilia. Moreover, while the shortening proceeds, the relative heights of the stereocilia in the staircase bundle are preserved, indicating that the depolymerization rates are also scaled to the length of the stereocilia. Therefore, the rate of paracrystal disassembly appears to be independently regulated from actin polymerization.

We have no leads as to what controls disassembly at the base. However, we have made several observations that suggest a critical role for myosin XVa in stereocilia paracrystal elongation. Myosin XVa immunoreactivity is detected at the stereocilia tips from the earliest stages of stereocilia formation. Most strikingly, the immunoreactivity levels are proportional to the actin incorporation rates and are scaled to the length of the stereocilia within the bundle staircase. Myosin XVa immunoreactivity is concentrated in the confined region between the membrane and the barbed ends of the actin filaments of the paracrystal in the region where they insert or contact the tip density visualized by EM as an osmiophilic (electron-dense) structure at the tips of the stereocilia. It is not known what makes up the stereocilia tip density. However, the correlation of the shape and intensity of immunoreactivity for myosin XVa and the shape of electron density when comparing the tallest and the second rows of stereocilia as shown in Fig. 6 suggests that myosin XVa is part of this electron-dense structure or "tip complex." Myosin XVa could be work-

ing with other components of the tip complex, including capping and scaffold proteins, to regulate actin polymerization. The observation that the shaker 2J mice have very short stereocilia with rounded, symmetric tips lacking myosin XVa and the electron-dense structure is consistent with the potential role of myosin XVa in stereocilia paracrystal elongation.

Relationship of myosins VIIa and VI to a treadmilling stereocilia core

The side links between adjacent stereocilia, presumed to be important in determining the dynamic properties of the bundle, are highly ordered in the bundle's geometry. Recent biochemical data suggest that myosin VIIa can form associations with stereocilia lateral link and scaffold proteins (Boeda et al., 2002). We have confirmed the localization of myosin VIIa along the paracrystal surface in the confined space between the paracrystal and the stereocilia membrane. Previously, it was shown that myosins could move a cargo on the surface of the stereocilia paracrystal toward the barbed end of actin filaments (Shepherd et al., 1990). It is possible that myosin VIIa, localized alongside the actin paracrystal, could "walk" on the treadmill and dynamically maintain stereocilia links and possibly other stereocilia components in place as the actin paracrystal treadmills rearwards (Fig. 8 B). In contrast, myosin VI, which is a unique myosin because it moves toward the pointed end of actin filaments, was reported to be present around the rootlet of stereocilia (Steel and Kros, 2001). We have now shown that it is also present along the actin paracrystal. Little is known about how the actin paracrystal tapers and how the membrane constricts at the stereocilia base. Future studies are needed to further characterize the precise role of myosin VI and its possible role in either translocating components along the paracrystal or helping to shape and stabilize the tapered base of the stereocilia.

Role of actin paracrystal turnover in stereocilia repair

The dynamic regulation of the actin treadmill and the observation that the dwell time for actin subunits within a stereocilia will be roughly equivalent throughout a population of stereocilia with varying lengths could represent the basis for stereocilia repair after damage from overstimulation. A substantial loss of cross-bridges was observed in the stereocilia actin paracrystal after sound overstimulation and suggested that the recovery process would involve some type of reformation of the actin cross-bridges over a period of several days (Tilney et al., 1982). A subsequent overstimulation study reported much faster recovery times (Duncan and Saunders, 2000). Perhaps overstimulation could produce actin paracrystal disruption at different portions along the paracrystal including the base of the stereocilia where the actin paracrystal structure is much thinner. The renewal process we describe continuously replaces the entire actin paracrystal from the elongation locus at the stereocilia tip downwards. The time required to complete the repair would depend on the extent and location of disruption along the paracrystal structure. In summary, we have now introduced a view in which stereocilia components are continuously turned over and the ordered staircase structure is not completely predetermined during development but undergoes continuous remodeling that may facilitate recovery from injury.

Materials and methods

Antibodies

Affinity-purified polyclonal antibodies were developed in rabbits immunized with synthetic peptides (Princeton Biomolecules) matching the sequences of myosins VI (AIESRQARPTYATAMIL and ELNLEETGLTRKRGAEILPRQFEE) and VIIa (LPGQEGQAPSGFEBLERGR and RLQKALRNGSRKYPPHLV). The production and affinity purification of myosin XVa antibodies were performed as described previously (Anderson et al., 2000).

Organotypic cultures of rat and mouse inner ear tissue

Organotypic cultures of rat and mouse organ of Corti and vestibular sensory epithelia were prepared according to Sobkowicz et al. (1993). Postnatal day 0–4 rat (or mouse) pups were anesthetized using CO_2 and decapitated according to National Institutes of Health (NIH) guidelines, and their temporal bones were isolated and placed into L-15 media (GIBCO BRL). The dissected organ of Corti was divided into pieces for culturing. Subsequently, the vestibular system was dissected. Tissues were attached to a Cell Tak (BD Biosciences)–coated coverslip in a culture dish. Cultures were maintained at 37°C and 5% CO_2 in DME F-12 supplemented with 7% FBS containing 1.5 μg/ml ampicilin (GIBCO BRL). For the cytochalasin D experiments, cultures were incubated 8, 16, 24, and 32 h with DME F-12 media containing 1 μM cytochalasin D, from a 2-mM DMSO stock (Sigma-Aldrich). For the BAPTA (1,2-*bis*(*o*-aminophenoxy) ethane-N,N,N′,N′-tetraacetic acid, 4 Na) experiments, cultures were gently washed with L-15 media without calcium and 5 mM BAPTA (Calbiochem) was applied. After 10-min incubation at 37°C, BAPTA was washed out with DME F-12 media and cultures were placed back into the incubator for 2 h.

Cell transfection and immunofluorescence

Cultured auditory and vestibular hair cells were transfected with 1 μm of gold carrier on which plasmid DNA coding for β actin–GFP (BD Biosciences) and small espin-GFP (a gift from J. Bartles, Northwestern University, Chicago, IL; Chen et al., 1999) were precipitated. A Helios Gene Gun (Bio-Rad Laboratories) was used to shoot 1-μm gold particles coated with DNA. Cultures were fixed with 4% PFA in PBS for 1 h, permeabilized for 30 min with 0.5% Triton X-100 in PBS, and counterstained with rhodamine/phalloidin (Molecular Probes) for 30 min. BAPTA- and cytochalasin D–treated samples were prepared as described above and actin filaments were counterstained with Alexa Fluor 488/phalloidin (Molecular Probes). Immunolocalization of myosins was performed on cultures and freshly dissected tissues fixed in 4% PFA in PBS at RT as described previously (Liang et al., 1999). Fluorescence images were obtained with a confocal microscope (model LSM 510 [Carl Zeiss MicroImaging, Inc.] or model Ultraview [PerkinElmer]). The relative amounts of myosin XVa expressed at the tips of stereocilia was quantified by measuring the integrated pixel intensity of the fluorescence image in a 250-nm diameter circular area of interest placed on the tips of stereocilia of different rows using the NIH image program.

Tissue preparation for EM

Unfixed rat and mouse organs of Corti were finely dissected and rapidly frozen, freeze-substituted in 1.5% uranyl acetate in absolute methanol at −90°C, infiltrated with Lowicryl HM-20 resin at −45°C, thin sectioned, and immuno-gold labeled as described previously (Dumont et al., 2001). Thin sections and freeze-etching replicas were viewed and photographed with an electron microscope (model 922; Leo). SEM of BAPTA-treated cultures and shaker 2J mice tissues (The Jackson Laboratory) were prepared as described previously (Anderson et al., 2000).

We thank Ulysses Lins for help with preliminary experiments and Ronald Petralia and Harrison Lin for comments on the manuscript.

Submitted: 13 October 2003
Accepted: 10 February 2004

References

Anderson, D.W., F.J. Probst, I.A. Belyantseva, R.A. Fridell, L. Beyer, D.M. Martin, D. Wu, B. Kachar, T.B. Friedman, Y. Raphael, and S.A. Camper. 2000. The motor and tail regions of myosin XV are critical for normal structure and function of auditory and vestibular hair cells. *Hum. Mol. Genet.* 9:1729–1738.

Assad, J.A., G.M. Shepherd, and D.P. Corey. 1991. Tip-link integrity and me-

chanical transduction in vertebrate hair cells. *Neuron.* 7:985–994.

Bartles, J.R. 2000. Parallel actin bundles and their multiple actin-bundling proteins. *Curr. Opin. Cell Biol.* 12:72–78.

Boeda, B., A. El-Amraoui, A. Bahloul, R. Goodyear, L. Daviet, S. Blanchard, I. Perfettini, K.R. Fath, S. Shorte, J. Reiners, et al. 2002. Myosin VIIa, harmonin and cadherin 23, three Usher I gene products that cooperate to shape the sensory hair cell bundle. *EMBO J.* 21:6689–6699.

Chen, B., A. Li, D. Wang, M. Wang, L. Zheng, and J.R. Bartles. 1999. Espin contains an additional actin-binding site in its N terminus and is a major actin-bundling protein of the Sertoli cell-spermatid ectoplasmic specialization junctional plaque. *Mol. Biol. Cell.* 10:4327–4339.

Dumont, R.A., U. Lins, A.G. Filoteo, J.T. Penniston, B. Kachar, and P.G. Gillespie. 2001. Plasma membrane Ca^{2+}-ATPase isoform 2a is the PMCA of hair bundles. *J. Neurosci.* 21:5066–5078.

Duncan, R.K., and J.C. Saunders. 2000. Stereocilium injury mediates hair bundle stiffness loss and recovery following intense water-jet stimulation. *J. Comp. Physiol. [A].* 186:1095–1106.

Forscher, P., L.K. Kaczmarek, J.A. Buchanan, and S.J. Smith. 1987. Cyclic AMP induces changes in distribution and transport of organelles within growth cones of Aplysia bag cell neurons. *J. Neurosci.* 7:3600–3611.

Fujiwara, I., S. Takahashi, H. Tadakuma, T. Funatsu, and S. Ishiwata. 2002. Microscopic analysis of polymerization dynamics with individual actin filaments. *Nat. Cell Biol.* 4:666–673.

Hasson, T., P.G. Gillespie, J.A. Garcia, R.B. MacDonald, Y. Zhao, A.G. Yee, M.S. Mooseker, and D.P. Corey. 1997. Unconventional myosins in inner-ear sensory epithelia. *J. Cell Biol.* 137:1287–1307.

Hudspeth, A.J. 1997. How hearing happens. *Neuron.* 19:947–950.

Kachar, B., M. Parakkal, M. Kurc, Y. Zhao, and P.G. Gillespie. 2000. High-resolution structure of hair-cell tip links. *Proc. Natl. Acad. Sci. USA.* 97: 13336–13341.

Kennedy, H.J., M.G. Evans, A.C. Crawford, and R. Fettiplace. 2003. Fast adaptation of mechanoelectrical transducer channels in mammalian cochlear hair cells. *Nat. Neurosci.* 6:832–836.

Liang, Y., A. Wang, I.A. Belyantseva, D.W. Anderson, F.J. Probst, T.D. Barber, W. Miller, J.W. Touchman, L. Jin, S.L. Sullivan, et al. 1999. Characterization of the human and mouse unconventional myosin XV genes responsible for hereditary deafness DFNB3 and shaker 2. *Genomics.* 61:243–258.

Loomis, P.A., L. Zheng, G. Sekerkova, B. Changyaleket, E. Mugnaini, and J.R. Bartles. 2003. Espin cross-links cause the elongation of microvillus-type parallel actin bundles in vivo. *J. Cell Biol.* 163:1045–1055.

Mallavarapu, A., and T. Mitchison. 1999. Regulated actin cytoskeleton assembly at filopodium tips controls their extension and retraction. *J. Cell Biol.* 146: 1097–1106.

Mogilner, A., and G. Oster. 1996. Cell motility driven by actin polymerization. *Biophys. J.* 71:3030–3045.

Romand, R., A.E. Zine, and A. Hafidi. 1993. Ontogenesis of F-actin in hair cells. *Cell Motil. Cytoskeleton.* 25:213–222.

Schneider, M.E., I.A. Belyantseva, R.B. Azevedo, and B. Kachar. 2002. Rapid renewal of auditory hair bundles. *Nature.* 418:837–838.

Shepherd, G.M., D.P. Corey, and S.M. Block. 1990. Actin cores of hair-cell stereocilia support myosin motility. *Proc. Natl. Acad. Sci. USA.* 87:8627–8631.

Sobkowicz, H.M., J.M. Loftus, and S.M. Slapnick. 1993. Tissue culture of the organ of Corti. *Acta Otolaryngol. Suppl.* 502:3–36.

Steel, K.P., and C.J. Kros. 2001. A genetic approach to understanding auditory function. *Nat. Genet.* 27:143–149.

Tilney, L.G., J.C. Saunders, E. Egelman, and D.J. DeRosier. 1982. Changes in the organization of actin filaments in the stereocilia of noise-damaged lizard cochleae. *Hear. Res.* 7:181–197.

Tilney, L.G., E.H. Egelman, D.J. DeRosier, and J.C. Saunder. 1983. Actin filaments, stereocilia, and hair cells of the bird cochlea. II. Packing of actin filaments in the stereocilia and in the cuticular plate and what happens to the organization when the stereocilia are bent. *J. Cell Biol.* 96:822–834.

Tilney, L.G., P.S. Connelly, L. Ruggiero, K.A. Vranich, and G.M. Guild. 2003. Actin filament turnover regulated by cross-linking accounts for the size, shape, location, and number of actin bundles in *Drosophila* bristles. *Mol. Biol. Cell.* 14:3953–3966.

Tyska, M.J., and M.S. Mooseker. 2002. MYO1A (brush border myosin I) dynamics in the brush border of LLC-PK1-CL4 cells. *Biophys. J.* 82:1869–1883.

Volkmann, N., D. DeRosier, P. Matsudaira, and D. Hanein. 2001. An atomic model of actin filaments cross-linked by fimbrin and its implications for bundle assembly and function. *J. Cell Biol.* 153:947–956.

Wanger, M., T. Keiser, J.M. Neuhaus, and A. Wegner. 1985. The actin treadmill. *Can. J. Biochem. Cell Biol.* 63:414–421.

Wegner, A. 1976. Head to tail polymerization of actin. *J. Mol. Biol.* 108:139–150.

Zheng, L., G. Sekerkova, K. Vranich, L.G. Tilney, E. Mugnaini, and J.R. Bartles. 2000. The deaf jerker mouse has a mutation in the gene encoding the espin actin-bundling proteins of hair cell stereocilia and lacks espins. *Cell.* 102: 377–385.